Fabric analyses of fine-grained glacier salt (Kuh-e-Namak, Dashti, southern Iran)

Julia Schmitz[1], Prokop Závada[2], Janos L. Urai[1]

[1] *Tectonics and Geodynamics Group, EMR, RWTH Aachen University*, [2] *Institute of Geophysics of the Czech Academy of Sciences, Czech Republic*

Motivation

Salt plays an important role in for the engineering industry for the search for a suitable nuclear waste disposal and caverns for gas storage but also in basin dynamics. Therefore, it is crucial to improve our understanding of deformation and recrystallization processes. Fine-grained salt in salt glaciers is weakened by influence of interstitial salt-brine solution enhancing solution-precipitation (SP) creep [2]. SP creep was already in 1979 proposed as the main reason for weakening glacier salt [1]. Therefore, glacier salt was proposed to flow at geologically high strain rates at very low shear stress down a slope in, for example, the Zagros Mountains and in Central Iran [3].

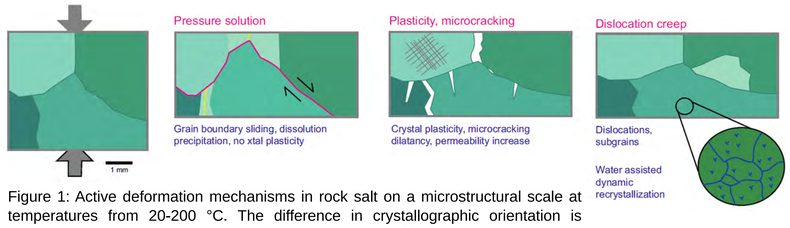

Figure 1: Active deformation mechanisms in rock salt on a microstructural scale at temperatures from 20-200 °C. The difference in crystallographic orientation is represented by different shades of green (from Urai et al., 2008).

Research questions

1. What constitutive flow laws can be used to describe salt rheology in fine-grained, mylonitic rock salt
2. Which different deformation mechanisms lead to grain size reduction?
3. How do they, together with the influx of rainwater and porosity, affect the creep of the salt mass in a regime where grain size sensitive solution-precipitation creep is dominant?

Quantitative Analyses

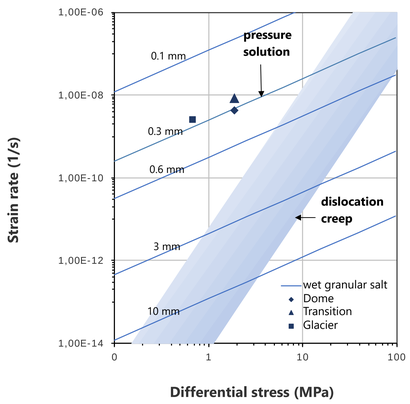

Figure 2: Stress-strain plot of the mean values for the Kuh-e-Namak (Dashti) glacier. Dome and transition are combined DC creep and SP creep, whereas the glacier for SP dominant. For the fine-grained glacier salt the total strain rate presents high values.

Table 1:
Parameters for shear stress calculations and resulting mean strain rate as a combination of dislocation creep and

Location	Thickness [m]	Angle [°]	Shear stress [MPa]	Mean total strain rate [s^{-1}]
Dome	100-250	20-45	0.37-1.91	4.23E-09
Transition	100-250	20-45	0.37-1.91	8.64E-09
Glacier	100-250	5-15	0.01-0.70	2.47E-09

Microstructures

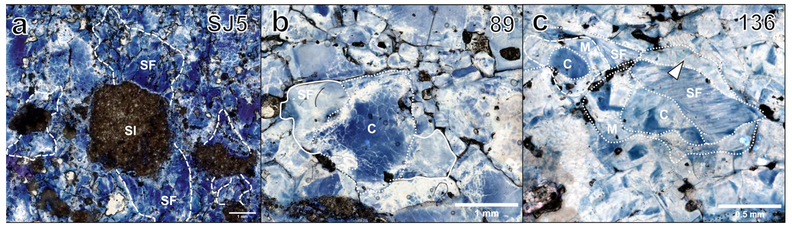

Figure 3: Micrographs of gamma-irradiated thinsections under transmitted light. a) Solid inclusions (SI) surrounded by fibrous halite in the strain fringes. Matrix grains show white substructures, b) Sample 89 reveal elongated subgrains from the core towards grain boundary in the rectangular growing grains in the strain fringes, c) core-mantle structures with fibrous strain fringes which have lobate grain boundaries to adjacent pale blue grains bulging into subgrain-rich grain.

Grain size reduction

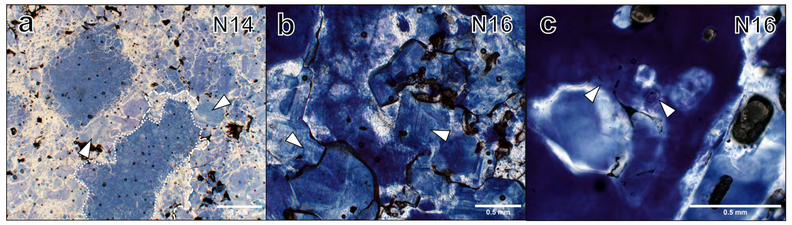

Figure 4: Grain boundary migration coupled with microcracking effectively decreases the grain size by different approaches: 1) subgrain-free grains bulging into subgrain-rich grains (Figure 3.3b,c, 3.4a,f, 3.5d-g); 2) nucleation of new grains at intragranular solid inclusions inside porphyroclasts (Figure 3.3e) dissection of porphyroclasts by grains grown by GBM (Figure 3.3a).

Porosity

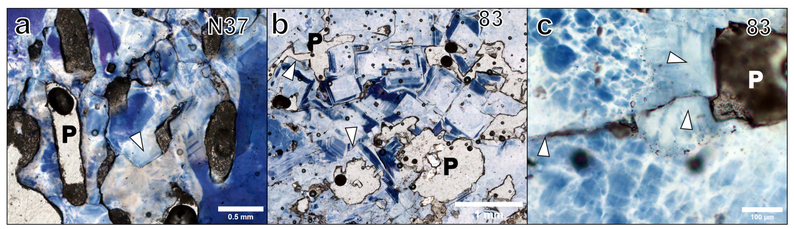

Figure 5: Micrographs under transmitted light of sample N37 and 83. a) Large elongated pores that are partially or filled by a solid phase. Arrow points toward a new grain boundary growing into pore space, b)shows sub- to euhedral grain growing in expense of the pore space, which is mostly filled by a solid phase, c) straight grain boundary segments growing from subgrain -rich grains into pores pace between those clasts and truncating each other. Growth directions are indicated by arrows. Left arrow shows small fluid inclusions between the two subgrain-rich grains.

EBSD

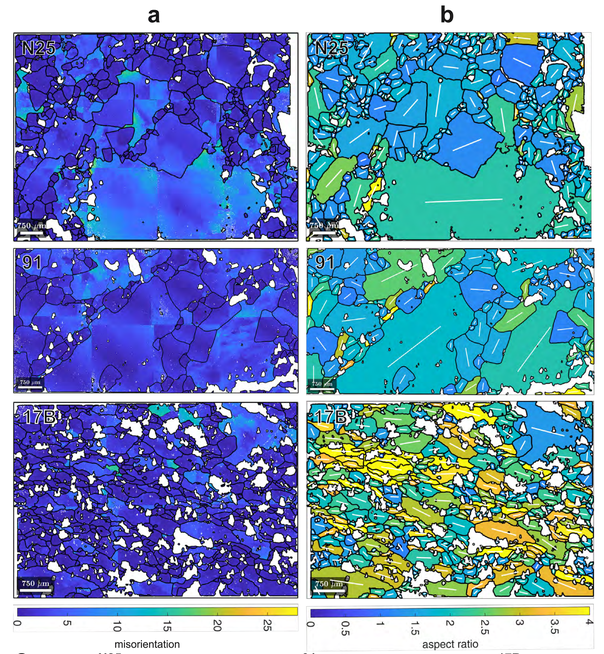

Figure 6: Misorientation, aspect ratio maps and rose diagrams reconstructed from EBSD data for samples N25, 91 and 17B. white areas are solid inclusions and porosity in the samples, a) column shows misorientation angle to the mean orientation of grains. b) Maps display the aspect ratio of each grain, whereas the white lines indicate the orientation of the long axis, c) rose diagrams of the three samples visualize the frequency of certain orientations of the long axis with the weighting of the size of the grains. Error created due to porphyroclasts that are cut off and it does not display their real orientation and aspect ratio. EBSD data shows an increase in elongation of grains while the amount of halite porphyroclasts and equiaxial matrix grains decreases. A strong SPO develops along the salt glacier profile.

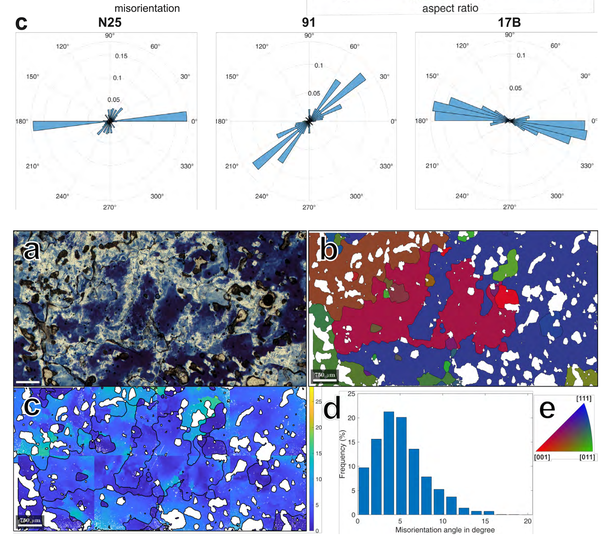

Figure 7: The domal sample N16 displays a bookshelf like structure due to recrystallization processes. a) transmitted-light micrograph of the porphyroclasts with the surrounding matrix grains, white bar indicated scale of 750 µm, b) reconstructed EBSD map of the average crystallographic orientationc) misorientation map displays the misorientation angle to the mean orientation, d) Histogram of frequency versus misorientation angle, e) Millersche Indizes and crystallographic orientation of grains in b).

Conclusion

1. Samples are dominated by solution-precipitation creep accompanied by grain boundary sliding, dislocation creep and grain boundary migration.
2. Microcracking under low stress is interpreted to be more active than in previous studies. We suggest that microcracking initiates dilatancy for the precipitation and development of abundant porosity in the samples by further leaching of water influx.
3. Effective grain size decreases by dismembering large halite porphyroclasts by three main processes of combined microcracking and grain boundary migration: 1) dissecting porphyroclasts ; 2) new grains growing in expense by bulging and 3) nucleation of new grains.
4. Differential stresses (1.9 – 6.1 MPa) inferred from subgrain piezometry (mean 14 – 99 µm).
5. Healed microcracks support the viscous behavior of the salt glacier and the incorporation of fluids into grain boundaries and grains.
6. Pore throats between pores seem to be recrystallized by precipitation of new material, which suggests an initially larger porosity.
7. Fine-grained salt (mean 118 – 508 µm), grain boundary fluids and the influx of meteoric water enhance deformation by solution-precipitation creep as in previous studies [4, 5].
8. Estimated strain rates in the order of magnitude 10^{-10} – 10^{-9} s^{-1} are geologically high creep rates representing the salt flow.

References [1] Wenkert, D. 1979. The Flow of Salt Glaciers. Geophysical Research Letters 6 (6): 523–26., [2] Urai, J.L., Spiers, C.J., Zwart, H.J. and Lister, G.S. 1986. Weakening of Rock Salt by Water During Long-Term Creep. Nature 324: 554–57, [3] Talbot, C.J. .1979. Fold trains in a glacier of salt in southern Iran. Journal of Structural Geology 1 (1), 5-18, [4] Urai, J. L., Spiers, C. J., Zwart, H. J., & Lister, G. S. (1986). Weakening of rock salt by water during long-term creep. Nature, 324(6097), 554–557. https://doi.org/10.1038/324554a0[5] Desbois, G., Závada, P., Schléder, Z., & Urai, J. L. (2010). Deformation and recrystallization mechanisms in actively extruding salt fountain: Microstructural evidence for a switch in deformation mechanisms with increased availability of meteoric water and decreased grain size (Qum Kuh,

Acknowledgments

Thanks to W. Kraus for the sample and thin section preparation and M. Racek for help with the EBSD measurements. Evaluation of the EBSD data with the MTEX toolbox M. Machek's help is kindly acknowledged.

EGU General Assembly | EMR | RWTH AACHEN UNIVERSITY